The CHESS Spectral Survey of Star Forming Region: Peering into the protostellar shock L1157-B1
I. Shock Chemical Complexity

Codella C. [1], Lefloch B.[2], Ceccarelli C.[2], Cernicharo J.[3], Caux E.[4], Lorenzani A.[1], Viti S.5,6, Hily-Blant P.[2], Parise B.[7], Maret S.[2], Nisini B.[8], Caselli P.[9,1], Cabrit S.[10], Pagani L.[10], Benedettini M.[6], Boogert A.[11], Gueth F.[12], Melnick G.[13], Neufeld D.[14], Pacheco S.[2], Salez M.[10], Schuster K.[12], Bacmann A.[2,15], Baudry A.[15], Bell T.[16], Blake G.[16], Bottinelli S.[4], Castets A.[2], Comito C.[7], Coutens A.[4], Crimier N.[2,3], Dominik C.[17,18], Demyk K.[4], Encrenaz P.[10], Falgarone E.[10], Fuente A.[19], Gerin M.[10], Goldsmith P.[20], Helmich F.[21], Henning Th.[22], Herbst E.[23], Jacq T.[15], Kahane C.[2], Kama M.[17], Klotz A.[2], Langer W.[20], Lis D.[16], Lord S.[16], Pearson J.[20], Phillips T.[16], Saraceno P.[6], Schilke P.[7,24], Tielens X.[25], van der Tak F.[21], van der Wiel M.[26,21], Vastel C.[4], Wakelam V. [15], Walters A.[4], Wyrowski F.[7], Yorke H.[20], Borys C.[16], Delorme Y.[10], Kramer C.[27], Larsson B.[28], Mehdi I.[20], Ossenkopf V.[24], Stutzki J.[24]

1: INAF, Osservatorio Astrofisico di Arcetri, Firenze, Italy 2: LAOG, Grenoble, France 3: CSIC, Madrid, Spain 4: CESR, Toulouse, France 5: UCL, London, UK 6: INAF-IFSI, Roma, Italy 7: MPIfR, Bonn, Germany 8: INAF-OAR, Monteporzio, Italy 9: University of Leeds, UK 10: IPAC, Pasadena, USA 11: LERMA, Meudon, France 12: IRAM, Grenoble, France 13: CfA, Cambridge, USA 14: Johns Hopkins University, Baltimore, USA 15: CNRS/INSU, Floirac, France 16: Caltech, Pasadena, USA 17: University of Amsterdam, The Netherlands 18: Department of Astrophysics/IMAPP, Nijmegen, The Netherlands 19: IGN-OAN, Madrid, Spain 20: JPL, Pasadena, USA 21: SRON, Groningen, The Netherlands 22: MPfA, Heidelberg, Germany 23: Ohio State University, Columbus, USA 24: Universität zu Köln, Germany 25: Leiden University, The Netherlands 26: Kapteyn Astronomical Institute, Groningen, The Netherlands 27: IRAM, Granada, Spain 28: Stockholm University, Sweden

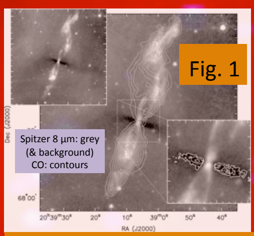

Fig. 1

Bachiller et al. (2001), Looney et al. (2007), Neufeld et al. (2009), Codella et al. (2009)

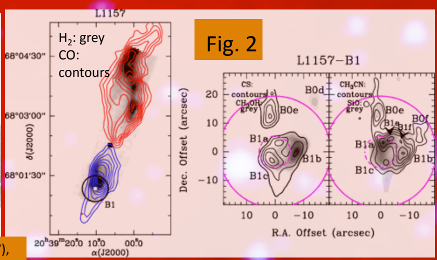

Fig. 2

The chemical active outflow L1157

The L1157 outflow, located at a distance estimated between 250 pc and 440 pc may be regarded as the ideal laboratory to observe the effects of shocks on the gas chemistry, being the archetype of the so-called chemically rich outflows. The low-luminosity (4-11 $L_\odot$) Class 0 protostar drives a precessing molecular outflow associated with several bow shocks seen in CO and in H_2. The brightest blue-shifted bow-shock, called B1 (Figs. 1-2), has been mapped with the PdB and VLA arrays revealing a rich and clumpy structure, the clumps being located at the wall of the cavity with an arch-shape (Tafalla & Bachiller 1995, Benedettini et al. 2007, Codella et al. 2009).

L1157-B1 is well traced by molecules released by dust mantles such as H_2CO, CH_3OH, and NH_3 as well as typical tracers of high-speed shocks such as SiO. Temperatures in the 60-200 K range are derived (e.g. Nisini et al. 2007). However, a detailed study of the excitation conditions of the B1 structure is still missing due to the limited range of excitation covered by the cm- and mm-observations performed so far. Observations of sub-mm lines with high excitation (> 50-100 K) are required. As part of the Herschel Key Program CHESS, L1157-B1 is currently investigated with an unbiased spectral survey using HIFI. We report here the first results based on the 555-636 GHz observations, revealing different molecular components at different excitation conditions coexisting in the B1 bow structure.

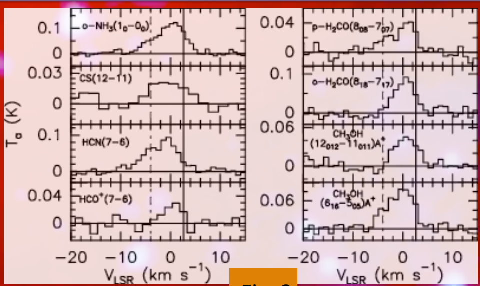

Fig. 3

Different tracers at different velocities

A total of 27 emission lines have been detected, with a wide range of upper level energies, up to a few hundred of K (Table 1). CO and H_2O are discussed in Lefloch et al. poster. Previous PdBI observations showed that L1157-B1 is associated with very high velocities (HVs) down to -20 km/s (Vsys = +2.6 km/s). The lack of detected emission in the HV regime in the present HIFI spectra could be due to the relatively low S/N ratio. Indeed, the PdBI images indicate that the brightness of the HV regime is weaker than the emission at low velocities by a factor of 5-10. The spectra in Fig. 3 show that a similar emissio could lie below the noise. Note that the HV emission is mostly confined within the eastern B1a clump (Fig. 2), in an emitting region with size 10", whereas low velocity lines originate in the bow-structure and in the walls of the outflow cavity, on a typical size of 15"-18". The forthcoming HIFI-CHESS observations at higher frequencies and at higher spatial resolution (dashed circle in Fig. 2) should allow us to study the HV wings in species other than CO and H_2O.

Table 1

Transition	ν_0^a (MHz)	E_u^a (K)
o-$H_2O(1_{10}-1_{01})$	556936.002	27
CH_3OH E $(11_{2,9}-10_{1,9})$	558344.500	168
o-$H_2CO(8_{18}-7_{17})$	561899.318	118
CH_3OH E $(3_{2,2}-2_{1,2})$	568566.054	32
o-$NH_3(1_0-0_0)$	572498.068	28
CO(5-4)	576267.931	83
p-$H_2CO(8_{08}-7_{07})$	576708.315	125
CH_3OH A^- $(2_{2,1}-1_{1,0})$	579084.700	45
CH_3OH E $(12_{1,12}-11_{1,11})$	579151.003	178
CH_3OH A^+ $(12_{0,12}-11_{0,11})$	579459.639	181
CH_3OH A^+ $(2_{2,0}-1_{1,1})$	579921.342	45
CH_3OH E $(12_{2,10}-11_{2,9})$	580902.721	195
CH_3OH A^+ $(6_{1,6}-5_{0,5})$	584449.896	63
CS(12–11)	587616.240	183
CH_3OH A^+ $(7_{3,5}-6_{2,4})$	590277.688	115
CH_3OH A^- $(7_{3,4}-6_{2,5})$	590440.291	115
CH_3OH E $(9_{0,9}-8_{1,8})$	590790.957	110
o-$H_2CO(8_{17}-7_{16})$	600374.604	126
CH_3OH E $(4_{2,3}-3_{1,3})$	616979.984	41
HCN(7–6)	620304.095	119
HCO^+(7–6)	624208.180	119
CH_3OH A^- $(3_{2,2}-2_{1,1})$	626626.302	52
CH_3OH E $(13_{1,13}-12_{1,12})$	627170.503	209
CH_3OH A^+ $(13_{0,13}-12_{0,12})$	627558.440	211
CH_3OH A^+ $(3_{1,2}-2_{1,2})$	629140.493	52
CH_3OH A^+ $(7_{1,7}-6_{0,6})$	629921.337	79
o-$H_2CO(9_{19}-8_{18})$	631702.813	149

The present HIFI spectra reveal another velocity component (here called medium velocity, MV), previously unidentified, traced by a secondary peak around -4.0 km/s and well outlined by HCN(7-6). The MV peak is visible also in $NH_3(1_0-0_0)$ and in some lines of CH_3OH and H_2CO, but its occurrence does not show any clear trend with the choice of tracer of line excitation. No single-dish spectra had previously revealed such a spectral feature, while an inspection of the spectra observed at PdBI shows that the MV secondary peak as observed in a couple of lines of the $CH_3OH(2_K-1_K)$ series and only towards the western B1b clump (size 5").

Figure 4 shows the comparison between the profiles of the $NH_3(1_0-0_0)$ and $H_2CO(8_{17}-7_{16})$ lines with the $H_2O(1_{10}-1_{01})$ profile, where the S/N allows us such an analysis (MV and LV ranges). As a notable example, the NH_3/H_2O intensity ratio decreases by a factor about 5 moving towards higher velocities: just optical depth effects or real decrease in the abundance ratios? In the latter case, this could reflect different pre-shock ice compositions in the gas emitting the MV emission. Alternatively, this behavior is consistent with the speculation that NH_3 is released by grain mantles, whereas water is released by grain mantles and, in addition, copiously formed in the warm shocked gas by endothermic reactions, which convert all gaseous atomic oxygen into H_2O. Water abundance could be enhanced with respect to ammonia in the fast and warm (> 200 K) gas, which might explain why the H_2O wings are larger than those of NH_3, of CH_3OH and H_2CO, all species directly evaporated from dust grain mantles.

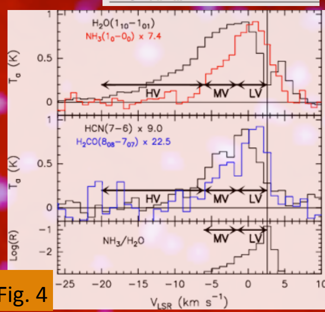

Fig. 4

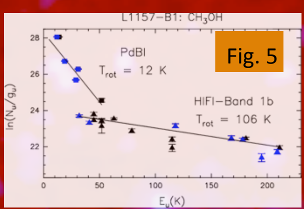

Fig. 5

Physical properties along the B1 bow shock

We derive a first estimate of the emitting gas temperature by means of the standard analysis of the rotational diagram. We show the case of methanol (A- and E-forms) in Fig. 5. The derived rotational temperature (Trot) is 106 K , a lower limit on the kinetic temperature. In the same figure we report the methanol lines (2_K-1_K) observed with PdBI and whose intensity is integrated in the HIFI 39" beam. The Trot derived by the ground-based data (based only on lines with Eu < 50 K) is definitely lower, 12 K, in agreement with that found with the 30-m spectra in the same excitation range. As discussed by Goldsmith & Langer (1999), this behavior could be due to the presence of two components at different temperatures or to non-LTE effects and line opacity. The two cases cannot be distinguished based only on the rotational diagram. Note that Nisini et al. (2010, in press) fit their H_2 rotation diagram with different slopes and thus different Trot, from 300 K to 1400 K .

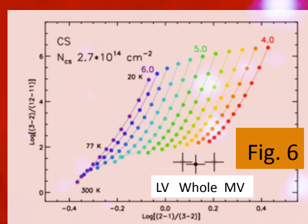

Fig. 6

Finally, if we combine the HIFI CS(12-11) line with CS(2-1) and (3-2) lines observed with ground based telescopes, we also derive with the LVG approach, a Tkin definitely above 300 K (Fig. 6). Caution should be taken since we could trace different gas components, as suggested by CH_3OH, the gas at higher excitation being traced by CS(12-11). If we analyse only the (2-1)/(3-2) intensity ratio, the LVG model does not allow one to give any constrain on Tkin, but we infer densities around 4 x 10^4 cm^{-3}. Interestingly, if we check a possible dependence of n_{H2} on velocity, the LV range indicates a denser medium (10^5 cm^{-3}) by an order of magnitude with respect to the MV gas. In conclusion, the present HIFI observations provide a sort of link between the gas at 60-200 K previously observed from ground and the warmer gas probed by the H_2 lines. Additional HIFI observations in the THz region are planned to be taken towards L1157-B1 to observe more species and transitions, carrying out the study of the different gas components associated with the bow structure.

References:
Bachiller et al. 2001 A&A 372 899 - Gueth et al. 1996 A&A 307 891
Benedettini et al. 2007 MNRAS 381 1127 - Looney et al. 2007 ApJ 670 L131
Codella et al. 2009 A&A 507 L25 - Nisini et al. 2007 A&A 462 163
Goldsmith & Langer 1999 ApJ 517 209 - Tafalla & Bachiller 1995 ApJ 443 L37